Adhesion between Immiscible Polymers Correlated with Interfacial Entanglements

Phillip J. Cole,† Robert F. Cook, and Christopher W. Macosko*

Department of Chemical Engineering and Materials Science, University of Minnesota, Minneapolis, Minnesota 55455

Received May 22, 2002

ABSTRACT: Adhesion in immiscible, weakly bonded polymeric layered structures is explored. Of particular interest are common commercial polymers used in multilayered packaging materials. Based on the scission of entangled chains at the polymer−polymer interface, a correlation between the critical mechanical energy release rate for fracture (G_c) and the characteristic number of interfacial entanglements (N_{ent}) is developed. N_{ent}, the ratio of the interfacial width to the average length scale required for entanglement, is calculable for a variety of homopolymers and random copolymers. Results of adhesion tests on melt and solvent laminated samples, coupled with random copolymer data from the literature, verify that a $G_c \propto N_{ent}^2$ relationship exists. For small N_{ent}, there are insufficient entangled chains to strengthen the interface, and the critical mechanical energy release rate goes to zero. The proposed model offers a method for designing new materials from common immiscible polymer systems.

Introduction

The control of polymer-to-polymer adhesion is important in a variety of applications. Multilayered polymeric composites typically fall into one of two categories. First, those that have only a few layers and function as a barrier or provide impact resistance.[1,2] As a specific example of adhesion control in this case, some carbonated beverage bottles have five polymeric layers that must remain adhered during use, yet be separable for recycling.[3] Second, they may consist of hundreds of submicron layers, possessing unique optical properties.[4,5] For polymeric composites with specialized optical behavior to retain an advantage over traditional materials, the layers must remain adhered when processed into unique shapes. Difficulties in providing these types of controlled adhesion have required alternative designs and have led to significant delays in manufacturing. Thus, understanding and predicting polymer-to-polymer adhesion remain critical issues in polymer composite design.

Most polymer pairs have a large positive enthalpy of mixing, resulting in macroscopic phase separation when blended. Therefore, it is expected that interface integrity would be weak in polymeric composites. A simple calculation of the work of adhesion (based on surface and interfacial energies) between two polymers is typically on the order of mJ/m^2;[6,7] however measured adhesion values are on the order of J/m^2.[8,9] This difference illustrates the important role of entanglements in providing adhesion in excess of van der Waals or hydrogen-bonding contributions. More explicitly, despite the immiscibility of most polymers, a narrow region of overlap between two polymers forms during melt or solvent processing. An infinitely sharp interface is not formed; rather, a transition region created, in which polymer chains of one type gradually decrease in density as polymer chains of a second type increase in density. An interphase is thus created that has a typical thickness of 1−5 nm. Within this interfacial region, long polymer chains of each type become entangled. Entanglements form readily in the melt or in solvent, where chains have sufficient mobility. As solvent is evaporated or molten samples cooled, entanglements are frozen in place, providing physical links. In this way, even immiscible polymers can adhere.

The number of entanglements that bond the interface is expected to depend in part on the breadth of the interfacial region. The width of the interface and its integrity are directly affected by varying the bonding temperature or the chemistry of the polymeric components. This has been confirmed in near-miscible systems, where slight changes in temperature can result in large differences in interfacial width.[10,11] However, such systems are rare, exhibiting much greater adhesion than most common polymer pairs. In this paper we measure adhesion of 11 polymer pairs and examine data on seven copolymers from the literature, in which the chemistry was instead varied. This permits the evaluation of a chain scission model for scaling adhesion in polymeric composites in which the adhesion is entanglement-based.

Scaling Analysis

In most polymeric composite systems in which entanglements are the primary source of adhesion, three adhesive failure mechanisms are active: chain scission, chain pullout, and crazing. Detailed descriptions of each of these failure processes are available elsewhere.[12,13] Figure 1 illustrates in which regime each of these mechanisms dominates. In the welding of a polymer to itself, the horizontal axis is molecular weight, and there is a transition from pullout to crazing as the chain length increases.[14] In laminating two immiscible polymers, the horizontal axis may instead be the interfacial width, and the transition is from scission (or pullout) to crazing.[15,16] An important consideration in the study of common multilayered polymer systems is determining

† Present address: Sandia National Laboratories, Albuquerque, NM 87111.

* To whom correspondence should be addressed.

10.1021/ma020789t CCC: $25.00
Published on Web 03/28/2003

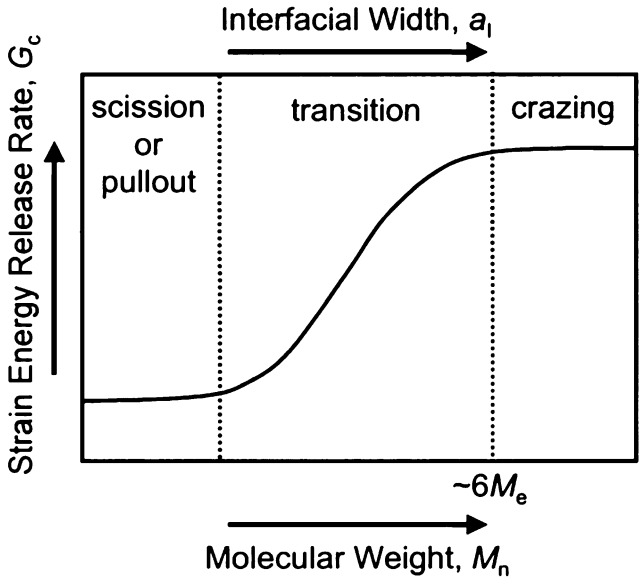

Figure 1. Schematic representation of the dramatic increase in adhesion that occurs as a result of a shift in failure mechanism. For miscible systems, as molecular weight increases to over $6M_e$, there is a transition from pullout to crazing. This is accompanied by a significant increase in the measured critical mechanical energy release rate. Similarly, for immiscible polymer pairs, as the interfacial width increases, a_I, there is a transition from scission (or pullout) to crazing.

which mechanism(s) is operating. Such systems contain high molecular weight components, which reduces the contribution from chain pullout. The remaining two mechanisms, scission and crazing, are related. The crazing process begins with the formation of microvoids and fibrils. As crazes grow, additional bulk material is drawn into the interfacial region.[17] Given sufficient tensile loading, the fibrils themselves fail through a scission event. Brown has developed a model for crazing that relates the critical mechanical energy release rate (G_c) to the areal density of entangled chains (Σ) and the crazing stress (σ_{cr}).[18] Equation 1 shows the proportionality between these parameters as predicted by Brown's model.

$$G_c \propto \frac{\Sigma^2}{\sigma_{cr}} \tag{1}$$

All interfaces between glassy polymers that have sufficient integrity to induce crazing are expected to conform to eq 1.[18] However, the interfaces in many layered polymeric composites are quite weak and mostly likely fail through a scission mechanism.

Chain scission can be described through comparison to other classes of materials, such as nonpolymeric crystalline solids. Consider two distinct layers bound together by a series of point contacts. These may represent chemical bonds of various types or physical bonds such as entanglements. If the two layers are subsequently separated, as shown in Figure 2, each of the point adhesion contacts must be broken before the crack tip can advance. Figure 2 provides a typical load−displacement curve for this type of process. The integrated area of this curve is the work done to separate a contact and in the simplest case is proportional to the work of adhesion (W_a). Equivalently, this is the resistance to fracture (R), which is composed of the work to

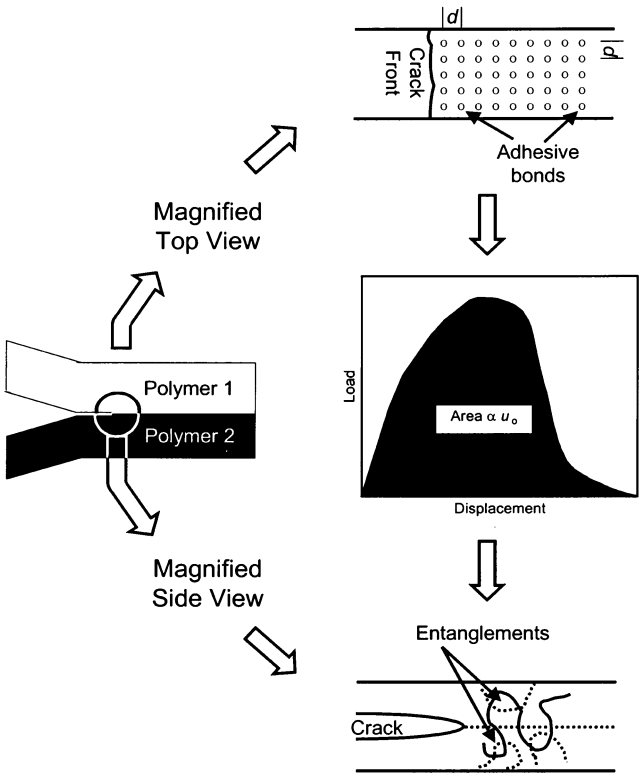

Figure 2. Magnified schematic views of the interfacial region showing the development of the scission model. (top view) A representation of a periodic array of adhesion contacts restraining the advancing crack front. (side view) A graphical demonstration of how entanglements bond the interface and the characteristic number that may be involved during crack propagation. Between the two magnified views is a typical load−displacement curve for the separation of a contact. The integrated area of the curve is proportional to the work done in separating the two layers.

fracture (u_0) each of the Σ bonds per unit of interfacial area, yielding

$$R = u_0\Sigma \tag{2}$$

If the bonds are equally spaced a distance d apart, as in a lattice, then eq 2 becomes

$$R \propto \frac{u_0}{d^2} \tag{3}$$

However, there is no requirement that the distance be a lattice parameter. Rather, it may be any distance representing the average spacing between the adhesion points. Using a characteristic distance λ to represent the spacing, eq 3 becomes

$$R \propto \frac{u_0}{\lambda^2} \tag{4}$$

For multilayered polymers, entanglements provide the adhesion through physical bonds. Therefore, the relevant λ is the spacing between entanglements. In a bulk polymer, this spacing can be calculated from the entanglement molecular weight. Analogous to the method of estimating polymer chain dimensions, the entanglement molecular weight can be converted to an entanglement length, L_e, through a radius of gyration expression as shown in eq 5.[11,13,19,20]

$$L_{e,i} = b_i\sqrt{\frac{M_{e,i}}{6M_{0,i}}} = b_i\sqrt{\frac{X_{e,i}}{6}} \tag{5}$$

In this equation, M_0 is the monomer repeat unit molecular weight, X_e is the entanglement degree of polymerization, and b is the statistical segment length of the polymer. L_e will vary depending on the characteristics of the polymeric components. For example, the pendant phenyl ring in polystyrene provides steric hindrance, limits free rotation along the backbone, and decreases the ability of polystyrene chains to form entanglements. In contrast, polyethylene has no such restrictions, resulting in a shorter distance between entanglement points and a smaller L_e. Thus, the i subscript indicates that the parameters are unique for each polymer. It should be noted that some literature has used a similar construct, the tube diameter (d_t), as defined by[16]

$$d_t = b_i\sqrt{\frac{4X_{e,i}}{5}} \tag{6}$$

Equations 5 and 6 differ by only a constant and therefore are expected to have identical scaling behavior.

The entanglements that directly affect the adhesion between immiscible polymers exist in the overlap region as discussed above. Helfand and Tagami have shown that the width of this interfacial region is[21]

$$a_I = 2\left[\frac{b_1^2 + b_2^2}{12\chi}\right]^{1/2} \tag{7}$$

where χ is the enthalpic interaction parameter. Statistical segment lengths have been measured or may be estimated for many polymers.[22,23] Similarly, χ values are available for a variety of polymer pairs, are measurable, or may be calculated using[24,25]

$$\chi = \frac{V_{ref}}{RT}(\delta_1 - \delta_2)^2 \tag{8}$$

where V_{ref} is an equivalent monomer reference volume, δ_i is the solubility parameter of polymer i, R is the gas constant, and T is the temperature. Thus, eq 7 is calculable for a variety of polymer systems.

The characteristic number of entanglements, N_{ent}, that provide physical links between two immiscible polymers is inversely proportional to their spacing. Further, entanglements are limited by the width of the interphase, such that

$$N_{ent} = \frac{a_I}{\overline{L_e}} \tag{9}$$

where $\overline{L_e}$ is the mean entanglement length scale for the polymer pair. As illustrated in the enlargement of the interfacial region in Figure 2, as a crack is propagated at the interface, entangled chains are broken. The resistance to fracture is then given by

$$R \propto \left(\frac{a_I}{\overline{L_e}}\right)^2 \propto N_{ent}^2 \tag{10}$$

The resistance to fracture is the interfacial adhesion, or equivalently at equilibrium, the critical mechanical energy release rate, resulting in

$$G_c \propto N_{ent}^2 \tag{11}$$

Combining eqs 5, 7, and 9 yields

$$N_{ent} = \left[\frac{2(b_1^2 + b_2^2)}{b_1 b_2 \chi (X_{e,1}X_{e,2})^{1/2}}\right]^{1/2} \tag{12}$$

For the special case of $b_1 = b_2$ and $X_{e,1} = X_{e,2}$, eqs 11 and 12 give

$$G_c \propto N_{ent}^2 \propto \frac{4}{\chi X_e} \propto \frac{4RT}{V_{ref}X_e(\delta_1 - \delta_2)^2} \tag{13}$$

While eq 12 is required to calculate N_{ent}, eq 13 suggests methods of evaluating the adhesion model. Specifically, differences in adhesion may be compared to those expected from altering the miscibility.

Experimental Section

Materials. The polymers used in this study are listed in Table 1. All were polydisperse, commercial polymers with large molecular weights. The molecular weight distributions were obtained through size exclusion chromatography, with the exception of the amorphous polyamide for which the manufacturer supplied the information in Table 1. The polymers were in pellet form, except for the PEO, which was a powder.

Sample Preparation. Polymers that were susceptible to water absorption were dried for at least 24 h prior to use. PMMA, PC, PET, and aPA were dried at 105 °C in a gravity convection oven, while PEO was dried at 50 °C in a vacuum oven. Each of the polymers was compression-molded in a press (Carver model AutoFour/30) to make plaques 2 cm wide and 7.5 cm long. The thickness (1−2 mm) of each polymer plaque was controlled using different thickness molds such that it was suitable for the adhesion test described below. After loading the mold, each sample was held at a temperature for 3 min to permit melting. A low pressure of approximately 0.7 MPa was applied for 2 min to cause the polymer to flow and fill the mold. Subsequently, while still in the melt, a high pressure of approximately 17 MPa was applied for 5 min. Prior to removing the samples, the press platens were water-cooled under pressure to room temperature. PE, PP, PEO, PMMA, PS, and PVC were pressed with the mold at 200 °C and between two sheets of Mylar film. aPA, PET, and PC were pressed with the mold at 220, 240, and 240 °C, respectively, using Teflon on one side of the mold and a polished steel plate on the other.

Bilayer samples were prepared through either a melt lamination or solvent lamination process using the 2 cm by 7.5 cm plaques. In the melt lamination, the procedure was identical to the plaque preparation, except that steel shims were used to control thickness instead of molds, and the high-pressure step was held for 10 min instead of 5 min. The press temperature was set to match the polymer with the highest processing temperature. For the polymer pairs at 220 or 240 °C, the interface was formed with the side of each plaque that had not been in contact with the Teflon. In some pairs the melt lamination caused flow around the sample edges. These were carefully removed with a hot-wire cutter. For the solvent lamination, each polymer layer was lightly coated with either dimethylformamide (aPA with PS) or tetrahydrofuran (all other solvent laminates), stacked together to form a bilayer, and pressed at room temperature under 34 MPa for 30 min. The solvent laminates were then left for 72 h to ensure complete diffusion and evaporation of the solvent.

Adhesion Testing. The bilayer adhesion was quantified through an asymmetric dual cantilever beam crack propagation (DCB) test as shown in Figure 3. In this adhesion test a razor blade of thickness Δ was driven into the interface

Table 1. Properties of Polymers Used in This Study

polymer	abbreviation	source	product no.	M_n (kg/mol)	M_w/M_n
amorphous nylon	aPA	DuPont	Zytel 330	25	~2.0
polycarbonate	PC	General Electric	Lexan 141	26	1.9
polyethylene	PE	Exxon	Exceed 350-D60	50	2.3
poly(ethylene oxide)	PEO	Aldrich		135	~2.2
poly(ethylene terephthalate)	PET	Aldrich		25	~2.6
poly(methyl methacrylate)	PMMA	Atofina	Plexiglas MI7	80	1.9
polypropylene	PP	Exxon	PP 4062	56	2.4
polystyrene	PS	Dow	Styron 685	110	3.3
poly(vinyl chloride)	PVC	Geon	Geon 87402	25	5.2

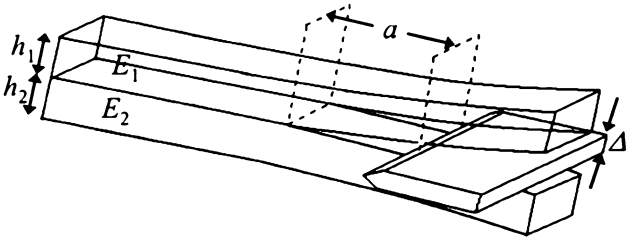

Figure 3. Schematic diagram of the asymmetric dual cantilever beam crack propagation (DCB) test. The modulus and thickness of each layer, as well as the crack length, are required for the calculation of the critical mechanical energy release rate. The crack length, a, is measured from the crack front to the tip of the wedge where the thickness is Δ.

between the two polymer layers to propagate an interfacial crack. After measuring the crack length, a, with a caliper and an optical microscope, the critical mechanical energy release rate, G_c, was calculated using eq 14 as described in the literature.[26,27]

$$G_c = \frac{3\Delta^2 E_1 E_2 h_1^3 h_2^3}{8a^4}\left[\frac{C_1^2 E_2 h_2^3 + C_2^2 E_1 h_1^3}{(C_1^3 E_2 h_2^3 + C_2^3 E_1 h_1^3)^2}\right] \quad (14)$$

where $C_i = 1 + 0.64(h_i/a)$, E_i is the modulus of layer i, and h_i is the thickness of layer i.

To obtain reliable data from the DCB test, additional points must be considered. First, the critical mechanical energy release rate is inversely proportional to the crack length raised to the fourth power, making the result very sensitive to the measurement of the crack length. Careful measurement and multiple data points are required for reasonable statistical analysis. In this study 8−10 measurements were made for each polymer pair, and the experimental uncertainty was taken as the standard deviation of all measurements. Second, as a crack is propagated with a single-edge razor blade, it may deviate into the more craze prone polymer layer.[28] This was avoided by varying the thickness ratio of the layers to find the minimum critical mechanical energy release rate, taken to be indicative of the true interface strength.[10] Third, as discussed previously, the focus of this investigation is on commercially viable multilayered structures, in which chain failure through a pullout mechanism can be largely eliminated.[14] For this reason, all polymers selected were high molecular weight, with number-average molecular weights greater than 6 times the entanglement molecular weight. Last, the DCB test was performed by propagating a crack, permitting the sample to equilibrate for 1 h, and measuring the resulting crack length. Thus, the measured G_c was an estimate of the equilibrium crack arrest value, independent of the initial rate of crack propagation and nonequilibrium values.[29] Each of these precautions is important if reliable adhesion results are to be obtained, and the critical mechanical energy release rates for different polymer pairs are to be compared.

Results

Effect of Molecular Weight. Prior to investigating the adhesion of a variety of polymer pairs, the effect of molecular weight on the critical mechanical energy release rate was confirmed. As mentioned previously, all of the polymers used in the adhesion study have an M_n greater than $6M_e$, with the PS and PMMA materials nearest this critical value. M_e for polystyrene is approximately 18 kg/mol and for PMMA is 13 kg/mol. Dai et al. have demonstrated the dependence of polymer fracture behavior on the number-average molecular weight, M_n.[30] Further, they observed a transition from chain pullout to chain scission at molecular weights equal to $5-8M_n$. Considering that $6M_e$ falls within this regime, the failure transition in PS and PMMA was studied.

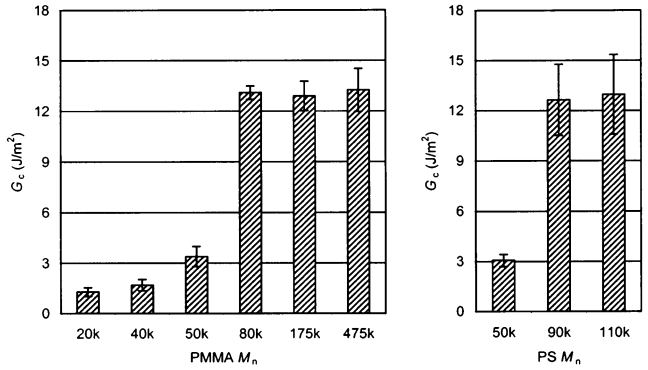

Figure 4. Adhesion results showing the influence of molecular weight. (a) Critical mechanical energy release rate data for the variation of PMMA molecular weight (g/mol) when laminated against PS. (b) Critical mechanical energy release rate data for the variation of PS molecular weight (g/mol) when laminated against PMMA.

Table 2. Polymers Used in the Determination of the Effect of Molecular Weight on Adhesion

	M_n (kg/mol)	M_w/M_n	source
Poly(methyl methacrylates) of Varying M_n			
1	20	2.3	Aldrich
2	40	2.0	Aldrich
3	50	2.1	Aldrich
4	80	1.9	Atofina
5	175	2.0	Aldrich
6	475	2.1	Aldrich
Polystyrenes of Varying M_n			
1	50	2.1	Dow 6690
2	90	2.3	Dow 666
3	110	3.3	Dow 685

First, the polystyrene listed in Table 1 was melt laminated with poly(methyl methacrylates) of different number-average molecular weights (M_n) summarized in Table 2. The results shown in Figure 4a indicate that the critical mechanical energy release rate (G_c) is only independent of molecular weight at an M_n of 80 kg/mol and greater. The data in Figure 4b were taken using the PMMA in Table 1 and polystyrenes of different M_n (Table 2), and a transition is observed between 50 and

Table 3. Calculated N_{Ent} and Adhesion Results for the Polymer Pairs Explored in This Study

	polymer 1	polymer 2	N_{ent}	G_c (J/m^2)	std dev[a]
melt	PP	aPA	0.38	0	
	PS	aPA	0.52	0	
	PS	PP	1.00	0	
	PS	PEO	1.03	4.5	0.6
	PS	PC	1.09	3.5	0.5
	PS	PVC	1.29	6.1	1.2
	PS	PE	1.44	9.5	0.8
	PS	PMMA	1.90	12.2	2.5
	PET	PC	2.44	21.3	2.7
solvent	PS	aPA	0.42	0	
	PS	PVC	1.22	5.9	1.8
	PC	PMMA	1.57	9.8	1.2
	PS	PMMA	1.80	11.6	2.2
	PMMA	PVC	2.14	13.9	3.2

[a] The standard deviation represents 8−10 samples.

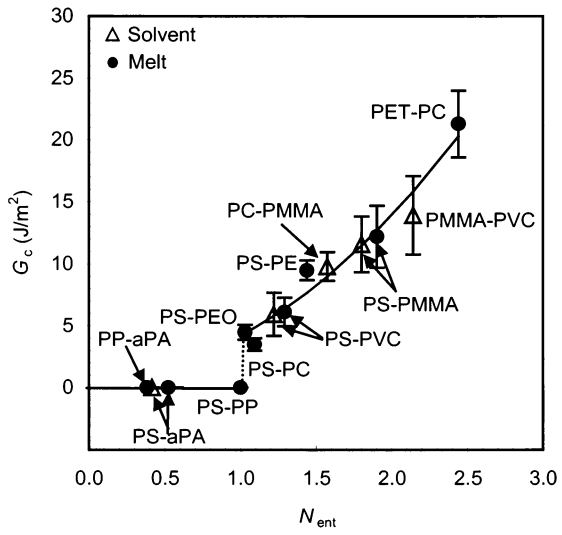

Figure 5. Adhesion data obtained using the DCB test. Solvent (Δ) and melt (●) laminated samples were prepared using the indicated polymer pairs. Error bars represent the standard deviation of 8−10 samples.

90 kg/mol. Thus, polymers with $6M_e$ demonstrated molecular weight independent behavior. Furthermore, the data are consistent with crack healing experiments, which demonstrated a similar polystyrene molecular weight was required to have molecular weight-independent properties.[14] This is also consistent with a transition from pullout to some form of bond rupture, such as scission or crazing, and is partial evidence that chain pullout is is expected to have a minimal contribution.

Thermal Contributions. After lamination and DCB testing, critical mechanical energy release rate data for 11 systems were obtained as shown in Table 3. The corresponding N_{ent} values were calculated using eqs 5, 7, 8, and 9, and the combined data are graphed in Figure 5. For small N_{ent}, the samples had insufficient adhesion to even test using the DCB technique. In melt laminates, differences in thermal expansion coefficients lead to residual thermal stress. This contribution was calculated through a method analogous to that of Sha et al.[31] In semicrystalline/amorphous melt laminates, differences in thermal expansion coefficients are larger, leading to areal strain energy densities of 1−2 J/m^2 upon cooling. This may have contributed to the zero values reported for the PP−PS (N_{ent} = 1.00) and PP−aPA (N_{ent} = 0.48) systems. However, residual thermal stresses alone cannot explain the results obtained with the aPA−PS system, in which both the melt and solvent laminates failed to show quantifiable adhesion. As the solvent laminates were prepared and tested at room temperature, there can be no thermal effects. Instead, the zero value must indicate insufficient entanglement. Collectively, the data at low N_{ent} suggest two limits. First, to have nonzero adhesion, a system must have $N_{ent} \geq 0.5$. PS−PEO, with $N_{ent} = 1.03$, had a G_c of 4.5 J/m^2. Yet PS−PP, in which $N_{ent} = 1.00$, had a critical mechanical energy release rate of zero. The only significant difference between these systems is in thermal expansion coefficient, with PS−PP being greater than PS−PEO. Thus, for the second limit, in which $N_{ent} \leq 1.0$, residual thermal stresses can induce delamination in melt laminates.

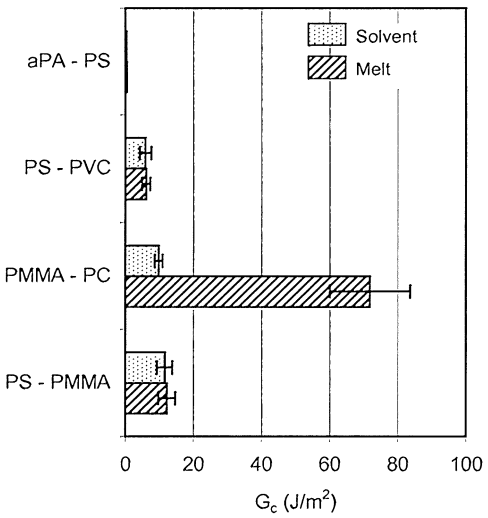

Figure 6. Direct comparison of solvent and melt laminated samples for four polymer systems. Three of the pairs show no difference in adhesion within the uncertainty of the measurement. However, PMMA−PC melt laminates have exceptionally large adhesion, likely as a result of interfacial reaction.

Laminates. Solvent and melt laminates were prepared for four polymer systems, including the aPA−PS samples discussed previously. The adhesion data have been included in Figure 5. The calculated N_{ent} for each melt sample is slightly larger than the solvent sample, because the processing temperature used in eq 8 is higher. Specifically, in the melt samples χ is reduced, a_I increases, and thus N_{ent} increases. However, all of the systems studied were relatively immiscible, such that the temperature difference did not considerably shift the χ value. Similarly, the adhesion did not change significantly, given the measurement uncertainty. This suggests that over a modest temperature range N_{ent} may be calculated at a single temperature (such as room temperature) and used for comparison purposes with negligible error. It is important to note that this would not be the case for near-miscible systems, for which small temperature changes may shift an immiscible system into the miscible range.

Figure 5 includes adhesion data from the systems that were both solvent and melt laminated, except for the PMMA−PC melt data. Figure 6 directly compares the lamination methods for these four systems and demonstrates a clear difference in the PMMA−PC system. A number of authors have shown that a possible interfacial reaction occurs between PMMA and PC.[32−35] Debier et al. have proposed that at elevated temperatures the ester bonds in PMMA can be hydrolyzed.[36] Subsequent

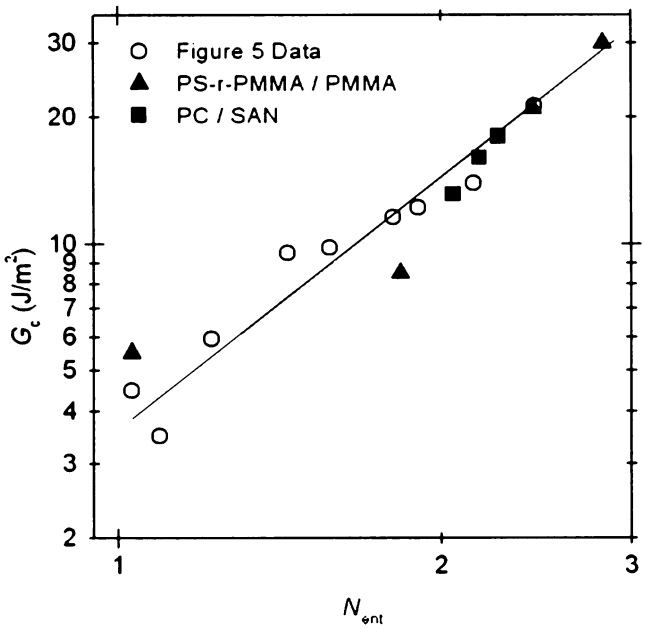

Figure 7. Comparison of literature and data from Figure 5 to a line of slope 2. The agreement suggests a relationship of the form $G_c \propto N_{ent}^2$ adequately describes the adhesion.

acidolysis of carbonate bonds in PC leads to the formation of a PC−PMMA copolymer. Further degradation of the PC can result in cross-linking of the system. The 7-fold increase in our melt adhesion data suggests that a reaction of the type they have suggested is in fact occurring. As this is a specialized case in which reaction can lead to enhanced adhesion and entanglements are not the primary source of adhesion, these data were excluded from Figure 5 and Table 3.

At $N_{ent} > 1$, adhesion increases with increasing N_{ent}, as demonstrated by the general trend of the experimental data in Figure 5. On the basis of the scission model leading to eq 11, a logarithmic plot of G_c vs N_{ent} should be linear with a slope of two. As shown in Figure 7, our data (open circles) are consistent with a line of slope two, verifying the $G_c \propto N_{ent}^2$ dependence. This is in part significant in that any polymer system that fails via a scission mechanism is expected to fit Figure 7.

Random Copolymers. Many applications benefit from the use of random copolymers instead of two separate homopolymers. Existing materials and the multitude of possible synthetic combinations make it desirable to investigate whether random copolymer data may be added to the homopolymer data presented above. For this reason, two sets of copolymer data from the literature have also been included in Figure 7. The triangles were adapted from adhesion data on a PMMA/PS-*r*-PMMA/PMMA system studied by Brown.[15] In this system the interfacial width was varied by altering the random copolymer (PS-*r*-PMMA) composition. The squares represent data from a PC/poly(styrene-*r*-acrylonitrile) (SAN) system. In this case, the SAN composition was varied, resulting in a change in the adhesion. The adhesion data were collected by Janarthanan et al.,[37] while the N_{ent} values were calculated on the basis of interfacial width data from Callaghan et al.[38] In the latter reference, two sets of interfacial width data were presented. The data that were found to be consistent with our calculations and with other literature[39] were used to calculate N_{ent}. As shown in Figure 7, the adhesion data for both copolymer systems show close agreement with the experimental data, supporting a $G_c \propto N_{ent}^2$ dependence.

The PMMA/PS-*r*-PMMA/PMMA system studied by Brown also demonstrates an important transition.[15] The complete data set resembles Figure 1, having chain scission and/or pullout dominating at small interfacial width. As the interfacial width increases above 80 Å, a transition to crazing occurs, and the measured adhesion increases markedly. Beyond 140 Å the critical mechanical energy release rate saturates, yielding a plateau value of approximately 250 J/m^2. Similar behavior has been observed in other polymeric composite systems.[16] Initially, the interface is weak, and there are insufficient entanglements to support the stress level required to initiate crazing. Since the transition represents a change in failure mechanism to crazing, it is expected to depend on the crazing stress, σ_{cr}. The crazing stress is polymer dependent; therefore, the exact transition point varies for each polymer system.[40] For the purposes of this discussion, the transition point provides the upper limit for the validity of the scission model, as the crazing stress was not included. For the crazing regime, the form of Brown's model (eq 1) is required.[18] While this is a limitation of our scission model, it is important to note that most polymer pairs form weak interfaces, never reaching the crazing regime.

Discussion

The agreement between the model and the data in Figure 7 emphasizes that eq 11 has captured the relevant physics. If there were a dependence on σ_{cr}, the data would not fall on a single line. It is also unlikely that the primary failure mechanism is chain pullout. This is in part due to the high molecular weight polymers used, as discussed above. There is additional evidence to support this hypothesis. If pullout were dominant, the stress required to induce chain pullout would be of the form

$$\sigma_{pullout} = \mu_{mono} N \Sigma \tag{15}$$

where μ_{mono} is monomeric friction coefficient, N is the degree of polymerization of the chain, and Σ is the areal density of chains undergoing pullout.[31,41] If μ_{mono} is polymer-specific, as suggested by Benkoski et al.,[16] then again the data would not fall on a single line.

For narrow interfacial regions, it may be possible to have pullout of unentangled loops of one polymer component. The transition from pullout to scission of loops has been shown to require twice the molecular weight of the corresponding linear chain.[41] Nevertheless, once the entanglement threshold is reached, scission or crazing would be favored over pullout. The stress contribution from the pullout of loops shorter than the entanglement length should be small, given the dependence on the degree of polymerization as shown in eq 15. Furthermore, the PMMA molecular weight data in Figure 4a indicate a transition in failure behavior in PS−PMMA laminates at 80 kg/mol, with higher molecular weights showing no molecular weight dependence. This would not be the case if pullout were still a significant factor, since eq 15 predicts a dependence on molecular weight. These data coupled with the lack of a dependence on the monomer-specific friction factor as shown in Figures 5 and 7 offer strong evidence that the pullout of loops is not a significant contributor. Although there should be a significant difference between the

friction coefficients for a polymer such as polystyrene compared to polyethylene, it is conceivable that the variations could be concealed within the adhesion measurement scatter. A more thorough mechanistic study would be required to completely eliminate the possibility of a contribution from pullout.

While it was not feasible in this study to offer direct visual evidence of a specific failure mechanism, the magnitudes of the critical mechanical energy release rates provide certain constraints. Specifically, the contribution of scission to the total G_c can be estimated. If the approximate number of interfacial bonds to be broken is $7.5 \times 10^{13}/\text{cm}^2$ based on the fracture of a pure polymer,[13,42] and an average bond energy is 80 kcal/mol (335 kJ/mol) for a carbon to carbon bond, then $G_{c,\text{scission}} \approx 0.4$ J/m^2.[13,43] An immiscible system should have significantly fewer bonds crossing the interfacial region, yielding an even smaller contribution from scission. Thus, simple bond-breaking cannot account for the critical mechanical energy release rates in Figure 7, ranging from 4 to 30 J/m^2. There must be some deformation extending beyond the interface as a crack is propagated. As Figure 2 implies, few failure processes occur without some plastic deformation. However, this does not automatically imply that crazing must be occurring. Crazing stresses for the polymers in this study are greater than the stresses generated during the DCB test. In addition, the PMMA/PS-*r*-PMMA/PMMA data plotted in Figure 7 include the maximum G_c reported in this study, yet still fall below the crazing transition shown schematically in Figure 1. An explanation consistent with the above discussion is that there is local deformation extending two to three entanglement lengths from the crack plane. As the crack propagates, energy is expended in deforming the chains near the interface and in rupturing the bonds of the entangled chains. If the deformation is highly localized, as we have suggested, there need not be a dependence on the polymer components, as there would be in the case of crazing.

There is, however, an additional implication of a localized deformation. If a region of two to three entanglement lengths is being stressed, the crystalline regions of semicrystalline/semicrystalline systems could be deformed as well. For example, in the polyethylene−polypropylene system, which has an interfacial width of approximately 4 nm, the reorientation of crystalline lamellae required during deformation has been claimed to be responsible for providing an interfacial strength exceeding that of the constituent polymers.[20,44] For this mechanism to operate, entangled chains must cocrystallize with each of the component polymers. A failure of this type is dependent on the crystallinity of the polymers and the stress required to deform the crystalline lamellae, neither of which is included in scission model presented above. Therefore, semicrystalline/semicrystalline adhesion data are not expected to conform to Figure 7.

Conclusions

The experimental results, for 11 different polymer pairs, lead to the primary conclusion that polymer-to-polymer adhesion depends on the square of the ratio of the interfacial width to the average length scale required for entanglement. Random copolymer data from the literature lend additional support to the $G_c \propto N_{ent}^2$ dependence. While some deformation localized within two to three entanglement lengths is likely, the scission model presented successfully fits the data, implying that the relevant parameters have been included. It is significant that a bond rupture model describes the adhesion between weakly bonded, immiscible polymers, since similar models have been used to explain failure processes in other classes of materials such as ceramics and metals.

There are, however, limitations on the applicability of the scission model. If the interface has sufficient integrity to induce crazing, the $G_c \propto N_{ent}^2$ relationship would be inadequate. In this case, the crazing stress would need to be included as in eq 1. Additionally, high molecular weight polymers (M_n greater than $6M_e$) are required to reduce the contribution from chain pullout. Should pullout occur, the monomeric friction coefficient would depend on the polymer components, which would also need to be accounted for in the failure model. Last, adhesion in semicrystalline/semicrystalline pairs that have entangled chains cocrystallized with the homopolymer crystalline lamellae would have a contribution from the deformation of the lamellae, which is also not included in the model presented.

Despite its limitations, the scission model provides a method of correlating adhesion to calculable parameters through N_{ent} and the $G_c \propto N_{ent}^2$ relationship. Within the low adhesion regime, the interfacial strength for commonly produced materials can be predicted, thus providing the basis for the design of superior composites. An adhesion cutoff was also established; specifically, at $N_{ent} \leq 0.5$ there were insufficient entanglements to provide quantifiable adhesion, and at $N_{ent} \leq 1.0$ thermal stress effects contribute to melt laminate debonding. Additional direct study of the failure mechanism might also yield a method of predicting the point of transition to crazing and provide another tool for polymeric composite design.

Acknowledgment. This work was supported in part by the MRSEC Program of the National Science Foundation under Award DMR-9809364, the 3M Company, and a Doctoral Dissertation Fellowship from the University of Minnesota Graduate School. The authors thank W. W. Gerberich for helpful discussion. Assistance with sample preparation and adhesion testing from A. Daiub, E. Quan, and Y. Shaw is also appreciated.

References and Notes

(1) Newman, R. O., Jr.; Schrenk, W. J. US Pat. 3 673 050, 1972.
(2) Hsieh, A. J.; Song, J. W. *J. Reinf. Plast. Compos.* **2001**, *20*, 239−254.
(3) A discussion of these structures was published in TricorBraun Spring 2000 newsletter (www.tricorbraun.com).
(4) Alfrey, T., Jr.; Gurnee, E. F.; Schrenk, W. J. *Polym. Eng. Sci.* **1969**, *9*, 400−404.
(5) Weber, M. F.; Stover, C. A.; Gilbert, L. R.; Nevitt, T. J.; Ouderkirk, A. J. *Science* **2000**, *287*, 2451−2456.
(6) Mangipudi, V.; Tirrell, M.; Pocius, A. V. *J. Adhes. Sci. Technol.* **1994**, *8*, 1251−1270.
(7) Pocius, A. V. *Adhesion and Adhesives Technology: An Introduction*; Hanser: New York, 1996.
(8) Kramer, E. J.; Norton, L. J.; Dai, C.-A.; Sha, Y.; Hui, C.-Y. *Faraday Discuss.* **1995**, *98*, 31−46.
(9) Cole, P. J.; Macosko, C. W. *J. Plast. Film Sheeting* **2000**, *16*, 213−222.
(10) Schnell, R.; Stamm, M.; Creton, C. *Macromolecules* **1998**, *31*, 2284−2292.
(11) Schnell, R.; Stamm, M.; Creton, C. *Macromolecules* **1999**, *32*, 3420−3425.
(12) Kramer, E. J.; Berger, L. L. *Adv. Polym. Sci.* **1990**, *91*, 1−68.

(13) Wool, R. P. *Polymer Interfaces Structure and Strength*; Hanser: New York, 1995.
(14) Wool, R. P.; Yuan, B. L.; McGarel, O. J. *Polym. Eng. Sci.* **1989**, *29*, 1340−1367.
(15) Brown, H. R. *Macromolecules* **2001**, *34*, 3720−3724.
(16) Benkoski, J. J.; Fredrickson, G. H.; Kramer, E. J. *J. Polym. Sci., Part B: Polym. Phys.* **2001**, *39*, 2363−2377.
(17) Brown, H. R. *J. Mater. Sci.* **1979**, *14*, 237−239.
(18) Brown, H. R. *Macromolecules* **1991**, *24*, 2752−2756.
(19) Yamamoto, T.; Furukawa, H. *Polymer* **1995**, *36*, 2393−2396.
(20) Chaffin, K. A.; Bates, F. S.; Brant, P.; Brown, G. M. *J. Polym. Sci., Part B: Polym. Phys.* **2000**, *38*, 108−121.
(21) Helfand, E.; Tagami, Y. *J. Chem. Phys.* **1972**, *56*, 3592−3601.
(22) Fetters, L. J.; Lohse, D. J.; Richter, D.; Witten, T. A.; Zirkel, A. *Macromolecules* **1994**, *27*, 4639−4647.
(23) Fetters, L. J.; Lohse, D. J.; Graessley, W. W. *J. Polym. Sci., Part B: Polym. Phys.* **1999**, *37*, 1023−1033.
(24) Grulke, E. A. In *Polymer Handbook*, 3rd ed.; Brandrup, J., Immergut, E. H., Eds.; Wiley: New York, 1989; p VII-519.
(25) Young, R. J.; Lovell, P. A. *Introduction to Polymers*, 2nd ed.; Chapman & Hall: London, 1991.
(26) Kanninen, M. F. *Int. J. Fract.* **1973**, *9*, 83−92.
(27) Xiao, F.; Hui, C.-Y.; Washiyama, J.; Kramer, E. J. *Macromolecules* **1994**, *27*, 4382−4390.
(28) Brown, H. R. *J. Mater. Sci.* **1990**, *25*, 2791−2794.
(29) Creton, C.; Brown, H. R.; Deline, V. R. *Macromolecules* **1994**, *27*, 1774−1780.
(30) Dai, C.-A.; Kramer, E. J.; Washiyama, J.; Hui, C.-Y. *Macromolecules* **1996**, *29*, 7536−7543.
(31) Sha, Y.; Hui, C. Y.; Kramer, E. J.; Hahn, S. F.; Berglund, C. A. *Macromolecules* **1996**, *29*, 4728−4736.
(32) Rincon, A.; McNeill, I. C. *Polym. Degrad. Stab.* **1987**, *18*, 99−110.
(33) Rabeony, M.; Hseih, D. T.; Garner, R. T.; Peiffer, D. G. *J. Chem. Phys.* **1992**, *97*, 4505−4511.
(34) Kyu, T.; Ko, C.-C.; Lim, D.-S.; Smith, S. D.; Noda, I. *J. Polym. Sci., Part B: Polym. Phys.* **1993**, *31*, 1641−1648.
(35) Montaudo, G.; Puglisi, C.; Samperi, F. *J. Polym. Sci., Part A: Polym. Chem.* **1998**, *36*, 1873−1884.
(36) Debier, D.; Devaux, J.; Legras, R. *J. Polym. Sci., Part A: Polym. Chem.* **1995**, *33*, 407−414.
(37) Janarthanan, V.; Stein, R. S.; Garrett, P. D. *Macromolecules* **1994**, *27*, 4855−4858.
(38) Callaghan, T. A.; Takakuwa, K.; Paul, D. R.; Padwa, A. R. *Polymer* **1993**, *34*, 3796−3808.
(39) Willett, J. L.; Wool, R. P. *Macromolecules* **1993**, *26*, 5336−5349.
(40) Williams, J. G. *Fracture Mechanics of Polymers*; John Wiley & Sons: New York, 1984.
(41) Dai, C.-A.; Jandt, K. D.; Iyengar, D. R.; Slack, N. L.; Dai, K. H.; Davidson, W. B.; Kramer, E. J.; Hui, C.-Y. *Macromolecules* **1997**, *30*, 549−560.
(42) Mohammadi, N.; Klein, A.; Sperling, L. H. *Macromolecules* **1993**, *26*, 1019−1026.
(43) Kerr, J. A. In *Handbook of Chemistry and Physics*, 72nd ed.; Lide, D. R., Ed.; CRC Press: Boston, 1991; pp 9−105.
(44) Chaffin, K. A.; Knutsen, J. S.; Brant, P.; Bates, F. S. *Science* **2000**, *288*, 2187−2190.

MA020789T